

STATISTICAL SHAPE MODELING OF CAM-TYPE FEMOROACETABULAR IMPINGEMENT

M.D. Harris¹, M. Datar², E. Jurrus³, C.L. Peters⁴, R.T. Whitaker⁵ and A.E. Anderson⁵

1. ABSTRACT

Cam femoroacetabular impingement (FAI) is characterized by a malformed femoral head that may cause shearing between the femur and acetabulum, leading to intra-articular damage and early hip osteoarthritis. Radiographic measurements are used to diagnose cam FAI, but provide only a planar view of the femoral head and often assume the ideal femur shape to be spherical. Statistical shape modeling (SSM) can be used to objectively compare complex 3D morphology without the need to assume ideal geometry. The objective of this study was to generate accurate 3D reconstructions of femoral heads and apply statistical shape modeling to quantify 3D variation and morphologic differences between control and cam femurs. Femurs from 33 controls and 15 cam FAI patients were CT scanned and 3D surfaces were generated by image segmentation. Correspondence particles were optimally positioned upon each surface using a gradient descent energy function. Resulting particle configurations were used to generate mean shapes for each group. Morphological differences were calculated as the distance between mean control and patient geometries. Differences were consistent with the location and approximate shape of cam lesions found intra-operatively. Deviations in mean shape between groups were pronounced at the anterolateral head-neck junction, where the mean cam femur protruded from the mean control femur by a maximum of 2.7mm. Sustained protrusions of ~1.0-2.5mm were distributed from the anterior-posterior midline of the femoral neck along the entire anterolateral head-neck junction and distally along the anterior section of the neck. Future work will refine our statistical shape modeling software to quantify, on a patient-specific basis, the severity of cam lesions for pre-operative planning.

2. INTRODUCTION

Femoroacetabular impingement is a recently described disease of the hip that is marked by reduced clearance between the femoral head and acetabulum due to morphologic abnormalities of the femur (termed cam FAI), acetabulum (termed pincer FAI), or both (termed mixed FAI)¹. Cam FAI is caused by a bony lesion on the femoral head or reduced concavity in the femoral head-neck junction, which may cause shearing between the femur and acetabulum thereby damaging articular cartilage and the acetabular labrum (Fig. 1).

¹PhD Candidate, Depts of Orthopaedics and Bioengineering, University of Utah, ²PhD Candidate, School of Computing, U. of Utah, ³Research Associate, Scientific Computing and Imaging Institute, U. of Utah, ⁴Professor, Scientific Computing and Imaging Institute and School of Computing, U. of Utah, ⁵Corresponding Author, Assistant Professor, Dept of Orthopaedics, Adjunct Assistant Professor, Depts of Bioengineering and Physical Therapy, U. of Utah, 590 Wakara Way, Salt Lake City, UT, USA

Currently, diagnosis of cam FAI is largely done using two-dimensional radiographic measurements of femur morphology². Such measures are useful for cursory detection of cam FAI but their reliability has been debated^{2,3}. In addition, there is no agreement on the range of values that should be considered normal. Furthermore, most radiographic measures give only a limited 2D description of femur morphology and do not provide quantitative information that translates well for preoperative planning (i.e. they cannot specify the exact location and extent of a lesion, nor the amount of bone that should be debrided to achieve a “normal” shape). If physicians could be provided with knowledge of the size and shape of a cam lesion, a more exact diagnosis, as well as detailed preoperative planning, may be facilitated.



Figure 1. Radiographs of subjects with healthy (left) and cam FAI (right) femurs. Circles indicate the anterolateral head-neck junction.

Three-dimensional (3D) reconstructions of femurs built from subject-specific computed tomography (CT) images can present femoral head morphology as a continuum. However, even most studies incorporating 3D femur reconstructions fall back upon the questionable assumption that a sphere is the ideal femoral head shape⁴. Statistical shape modeling (SSM) can be applied to 3D reconstructions to objectively compare complex morphology without the need to assume ideal geometry. Most SSM strategies use a point distribution model that allows representation of a class of shapes by the mean positions of a set of labeled points to describe geometric variation among shapes within a population^{5,6}. Application of the SSM method to cam FAI patients may facilitate improved diagnosis and pre-operative planning by allowing physicians to classify cam lesions of various shapes and sizes with respect to an objectively determined 3D “average” healthy and average cam FAI femurs.

The objective of this study was to generate accurate 3D reconstructions of femoral heads from volumetric CT images and apply statistical shape modeling to quantify 3D variation and morphologic differences between control and cam femurs.

3. METHODS

3.1 Subject Selection

Fifteen patients (14 male, 1 female) with symptoms of cam FAI consented to receive a CT arthrogram (IRB #10983). All patients had hip and groin pain during activity, tested positive during a clinical impingement exam, showed radiographic evidence of a cam lesion and/or reduced femoral head-neck offset, and underwent or were scheduled for hip preservation surgery to address cam FAI. CT scans were acquired using a Siemens SOMATOM 128 Definition CT Scanner. Tube voltage was 120 kVP with an acquisition matrix of 512 x 512, slice thickness of 1.0 mm, and pitch of 0.9 to 1.0. The baseline tube current was 250 mAs (CareDose used to minimize radiation exposure). The field of view covered both hips and varied between 300-400 mm.

Thirty-three control femurs (25 male, 8 female) were selected from a database of cadaveric specimens (IRB #11755). All control femurs were qualitatively screened for cartilage damage and bony abnormalities. Femurs were aligned anatomically in a GE High Speed CTI Single Slice Helical CT scanner. Slices were 1 mm thick with tube voltage at 100 kVP, a 512 x 512 acquisition matrix, tube current of 100 mAs, pitch of 1.0 and a 160 mm field of view.

Using the CT images, digitally reconstructed radiographs were generated to mimic the commonly used frog-leg lateral x-ray⁷. Radiographic description of possible cam lesions and head-neck concavity was completed for all subjects by measuring the alpha angle and head neck offset as adapted by Clohisy et al. for using the frog-leg lateral view⁷.

3.2 Three-Dimensional Reconstruction and SSM Preprocessing

The proximal femur to lesser trochanter was accurately segmented from the CT image data using Amira (v5.4, Visage Imaging, San Diego, CA) and validated threshold settings⁸ (Fig. 2). To improve resolution of the segmentation mask, CT images were up-sampled to 1536×1536, 0.3 mm thickness for patients and 1024×1024, 0.5 mm for controls. A sensitivity study of voxel sizes found that further up-sampling of either control or patient images did not appreciably alter the morphology of resulting 3D reconstructions. Reconstructed surfaces were triangulated and segmentation artifacts were removed by slightly smoothing surfaces using tools available in Amira. Femurs were aligned in Amira using a built-in iterative closest point algorithm to minimize the root mean square distance between surfaces.

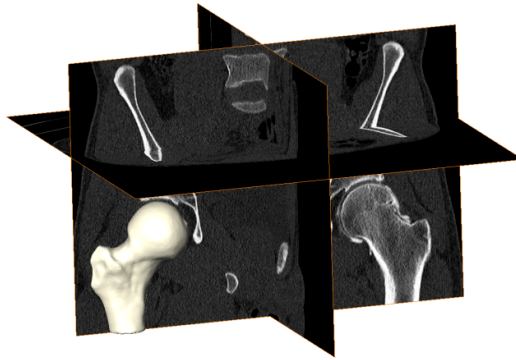


Figure 2. Volumetric CT images from a cam FAI patient. Validated threshold settings were applied to CT images to segment and reconstruct the bony morphology of each femur.

Surface reconstructions were then converted to binary segmentations (white = femur, black = exterior space) within a uniform bounding box with consistent voxel resolution of 512 x 512 x 400 (voxel size = 0.235 x 0.235 x 0.258 mm) for each femur.

3.3 Statistical Shape Modeling

The SSM method used has been described in detail by Cates et al.⁵. Briefly, a smooth surface is sampled using a set of N points, considered as random variables $\mathbf{Z} \sim (\mathbf{x}_1, \mathbf{x}_2, \dots, \mathbf{x}_N)^T$, where positions \mathbf{x} are *particles*. The method then iteratively moves a system of dynamic *particles* across the surfaces to find positions that optimize the information content of the system,

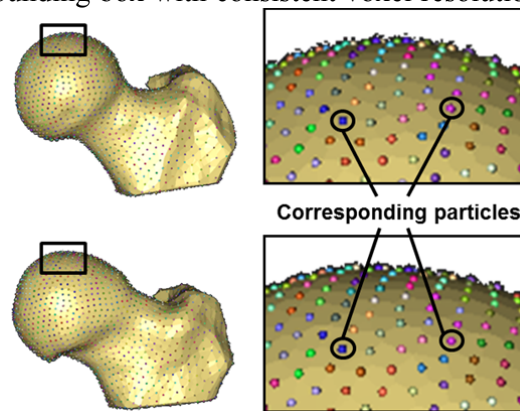


Figure 3. Correspondence particle distribution on a control and a cam FAI femur. 2048 particles were placed on each femur and optimally positioned to balance model compactness and accurate shape representation.

denoted by $H(\cdot)$. An ensemble comprised of M surfaces can be described by a $3N \times M$ matrix of particle positions $\mathbf{P} = (\mathbf{x}_j^k)$, where $k = 1, \dots, M$ and $j = 1, \dots, N$. Now, the combined ensemble and shape cost function is defined

$$Q = H(\mathbf{Z}) - \sum_k H(\mathbf{P}^k) \quad [1]$$

The first term of Q produces a compact distribution of samples in shape space, while the second term provides uniformly-distributed correspondence positions on the shape surfaces, to achieve a faithful shape representation. Binary segmentations of the femur were preprocessed to remove aliasing artifacts, and 2048 particles (aka *correspondences*) were initialized and optimized on each femur (Fig. 3), using a splitting strategy. The generalized Procrustes algorithm was applied during optimization to align shapes with respect to rotation and translation, and to normalize with respect to scale. Group labels were used to separate the point representation of controls and patients, and the mean shape for each group was constructed as the mean of the *correspondences* from all shapes belonging to that group.

3.4 Analysis

From optimized *correspondences*, mean shapes were generated to represent the average geometry of control and cam FAI femurs. A Hotelling T^2 test was used to test for group differences, with the null hypothesis that the two groups are drawn from the same distribution. Morphological differences were then calculated as the distance between mean control and cam geometries. Principal component analysis (PCA) was used to determine the co-ordinate system best suited for analysis of variation present in the selected population of femurs. Parallel analysis was used to project the correspondences into a lower dimensional space determined by choosing an optimal number of basis vectors from PCA.

4. RESULTS

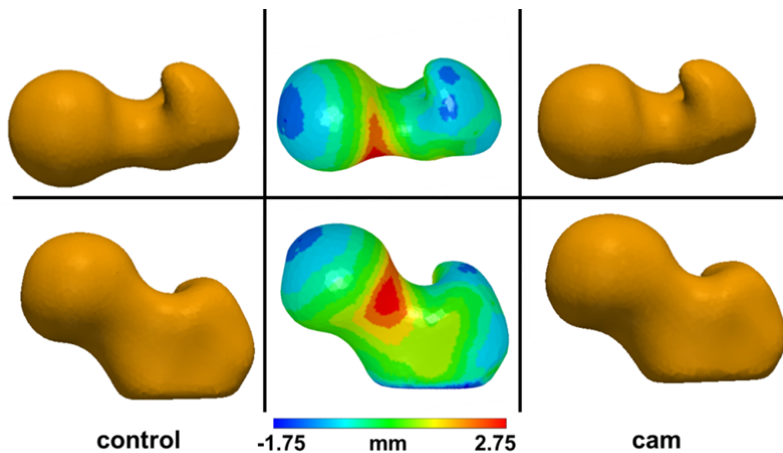


Figure 4. Mean control (left) and cam (right) shapes. Middle images show the mean control shape with color plots depicting how the mean cam shape differed across the femoral head, neck and proximal shaft. Top and bottom rows show different rotations of the femoral head.

The average and standard deviation age, weight, height, and BMI of the cam FAI patients were 26 ± 7 years, 83.0 ± 10 kg, 180.7 ± 7.7 cm, and 25.5 ± 3.3 kg/m², respectively. Alpha angles and head-neck offsets of the cam FAI patients were $71.9 \pm 13.2^\circ$ and 6.7 ± 1.4 mm, respectively. For controls, the average and standard deviation age, weight, height, and BMI were 32.4 ± 10.9 years, 85.2 ± 19.9 kg, 176.3 ± 9.9 cm, and 27.5 ± 6.8 kg/m². Alpha angles and head-neck offsets for the control femurs were $39.8 \pm 4.9^\circ$ and 9.0 ± 1.2 mm, and fell within previously reported values for

asymptomatic subjects^{7,9}.

The Hotelling T² test demonstrated significant differences between the control and cam FAI group mean shapes ($p = 0.002$). Morphologically, the mean cam FAI shape was found to protrude above the control mean by a maximum of 2.69 mm in the anterolateral head-neck junction (Fig. 4). Sustained protrusions of ~ 1.0 -2.5 mm were distributed from the anterior-posterior midline of the femoral neck along the entire anterolateral head-neck junction and distally along the anterior neck.

From parallel analysis it was determined that the first 6 modes (or components) from PCA captured non-spurious information for statistical comparison. Those 6 modes, captured 84.6% of the cumulative variation among the ensemble of femurs. Specifically, mode 0 captured 42.4% of the variation, with mode 1 capturing 22.9%, mode 2 capturing 8.6%, mode 3 capturing 5.1%, mode 4 capturing 3.1%, and mode 5 capturing 2.5% of the variation, respectively. Qualitative descriptions of variation captured by the first 3 modes are shown in Figure 5.

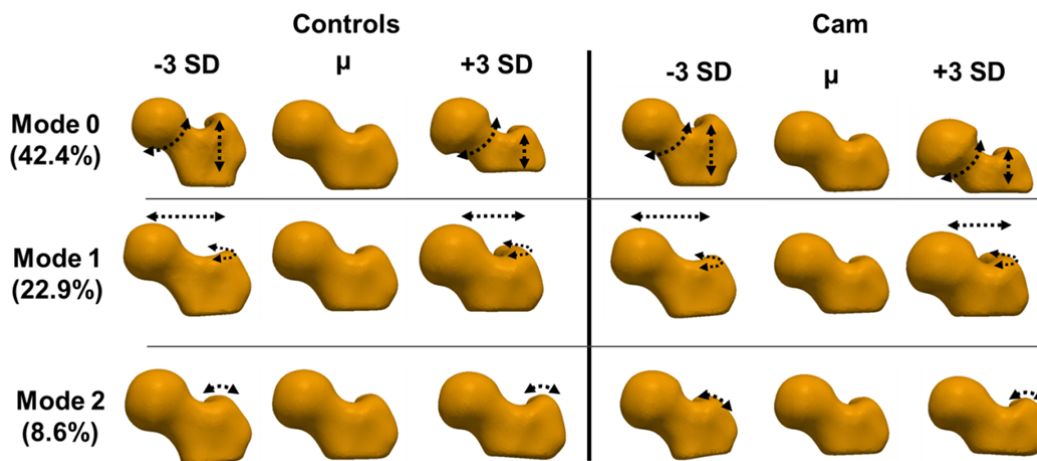


Figure 5. Mean shapes (μ) for both groups and shapes at ± 3 standard deviations for the first 3 modes. For both groups, mode 0 captured variation in head-neck concavity and distance between greater and lesser trochanters; mode 1 captured neck extension and anteroposterior curvature of the greater trochanter; mode 2 primarily captured coronal curvature of the greater trochanter.

5. DISCUSSION

In this study, statistical shape analysis was used to quantify and compare femoral head morphology between normal controls and cam FAI patients. Prior orthopaedic applications of SSMs have included analyses of tibiofemoral and patellofemoral joint shape with respect to osteoarthritis and knee pain, or to femoral shape with respect to neck fracture¹⁰⁻¹². However, to our knowledge, our study is the first application of SSM to quantify and characterize morphological differences between control and cam FAI femurs.

The primary result of this study was the computation of mean femoral shapes for controls and cam FAI patients. The greatest differences between the mean shapes were located along the anterolateral head-neck junction (Fig 4.), which corresponds very well with clinical findings of cam lesions locations and intraoperative findings of damage to the articular cartilage and labrum^{13,14}. The mean shapes, as well as color plotted

differences of individual cam femurs compared to the mean shapes, can serve as a quantitative “road map” for the location and amount of debridement required to restore a cam femur to a normal shape.

The majority of variation for the femur groups, as captured in mode 0, was in the contour of the head-neck junction and the distance between the greater and lesser trochanter. Variation at the head-neck junction suggests that while control and cam femurs are distinctly different in that region, there may be considerable differences even among control femurs with healthy head-neck offset or cam femurs with reduced offset. Interestingly, even cam femurs showed large head-neck offset at +3 standard deviations in mode 0. Computationally, this may have been influenced by the disproportionate number of control vs cam femurs analyzed. Alternatively, the current sample size of cam femurs may not be sufficiently large to capture all the variation that may exist among cam FAI patients. Thus, the number of cam femurs will be increased and cam femurs will be analyzed independently to determine if the morphological variation changes considerably. Variation in the distance between trochanters has not been shown previously to have any effect on the biomechanics of FAI, and may be secondary to size variation among femurs that was accounted for during Procrustes alignment. Having information about where variations among control and cam femurs (Fig. 5) are most common could further help physicians classify unusual FAI cases and aid in tailoring surgical intervention to individual subjects.

Until recently, most SSM correspondences for shape statistics were established manually by choosing small sets of anatomically significant landmarks on regions of interest, which would then serve as the basis for shape analysis⁶. The demand for more detailed analyses on ever larger populations of subjects has rendered this approach increasingly difficult. The current study used a method presented by Cates et al. for extracting dense sets of correspondences that describe large ensembles of similar shapes⁵. Thus instead of a reliance on relatively few correspondences or the necessity for training shapes, correspondence positions in this study resulted in a geometrically accurate sampling of individual shapes, while computing a statistically simple model of the ensemble. Because of this advantage over previous SSM techniques, we are easily able to increase the number of correspondences used and the number of femurs included in the analysis, both of which are part of our future work.

Cam FAI can be painful and has the potential to shorten the lifetime of a native hip through degeneration of articular cartilage and separation of the cartilage from the acetabular labrum¹³. Current hip preservation surgeries seek to mitigate damage by removing cam lesions and increasing head-neck concavity^{14,16}. Under correction of a cam lesion may cause lingering pain and could require revision surgery, while over correction could endanger the mechanical integrity or blood supply of the femur¹⁷. The use of statistical shape modeling with control and cam FAI femurs, as done in the current study, allows physicians to visualize individual cam lesions in context with average normal and pathologic shapes. Our control and cam femur databases are continually growing, thus improving the strength of the statistically determined shapes. SSM of cam FAI avoids the assumption that healthy femurs are spherical and allows objective determination of true femoral shape among normal and pathologic populations. Use of SSM of cam FAI in the clinical setting could improve not only our understanding of femoral morphology but may provide more exact diagnoses and improved pre-operative planning.

6. REFERENCES

1. Ganz, R., Parvizi, J., Beck, M., Leunig, M., Notzli, H., Siebenrock, K. A. Femoroacetabular impingement: a cause for osteoarthritis of the hip. *Clin Orthop Relat Res.* 2003 Dec(417): 112-120.
2. Clohisy, J. C., Carlisle, J. C., Trousdale, R., Kim, Y. J., Beaulé, P. E., Morgan, P., et al. Radiographic evaluation of the hip has limited reliability. *Clin Orthop Relat Res.* 2009 Mar;467(3): 666-675.
3. Barton, C., Salineros, M. J., Rakhra, K. S., Beaulé, P. E. Validity of the alpha angle measurement on plain radiographs in the evaluation of cam-type femoroacetabular impingement. *Clin Orthop Relat Res.* 2011 Feb;469(2): 464-469.
4. Audenaert, E. A., Baelde, N., Huysse, W., Vigneron, L., Pattyn, C. Development of a three-dimensional detection method of cam deformities in femoroacetabular impingement. *Skeletal Radiol.* 2011 Jul;40(7): 921-927.
5. Cates, J., Fletcher, P. T., Styner, M., Shenton, M., Whitaker, R. Shape modeling and analysis with entropy-based particle systems. *Inf Process Med Imaging.* 2007;20: 333-345.
6. Cootes, T. F., Taylor, C. J., Cooper, D. H., Graham, J. Active Shape Models-Their Training and Application. *Computer Vision and Image Understanding.* 1995;61(1): 38-59.
7. Clohisy, J. C., Nunley, R. M., Otto, R. J., Schoenecker, P. L. The frog-leg lateral radiograph accurately visualized hip cam impingement abnormalities. *Clin Orthop Relat Res.* 2007 Sep;462: 115-121.
8. Anderson, A. E., Peters, C. L., Tuttle, B. D., Weiss, J. A. Subject-specific finite element model of the pelvis: development, validation and sensitivity studies. *J Biomech Eng.* 2005 Jun;127(3): 364-373.
9. Pollard, T. C., Villar, R. N., Norton, M. R., Fern, E. D., Williams, M. R., Simpson, D. J., et al. Femoroacetabular impingement and classification of the cam deformity: the reference interval in normal hips. *Acta Orthop.* 2010 Feb;81(1): 134-141.
10. Bredbenner, T. L., Eliason, T. D., Potter, R. S., Mason, R. L., Havill, L. M., Nicolella, D. P. Statistical shape modeling describes variation in tibia and femur surface geometry between Control and Incidence groups from the osteoarthritis initiative database. *J Biomech.* 2010 Jun 18;43(9): 1780-1786.
11. Bryan, R., Mohan, P. S., Hopkins, A., Galloway, F., Taylor, M., Nair, P. B. Statistical modelling of the whole human femur incorporating geometric and material properties. *Med Eng Phys.* 2010 Jan;32(1): 57-65.
12. Fitzpatrick, C. K., Baldwin, M. A., Laz, P. J., FitzPatrick, D. P., Lerner, A. L., Rullkoetter, P. J. Development of a statistical shape model of the patellofemoral joint for investigating relationships between shape and function. *J Biomech.* 2011 Sep 2;44(13): 2446-2452.
13. Beck, M., Kalhor, M., Leunig, M., Ganz, R. Hip morphology influences the pattern of damage to the acetabular cartilage: femoroacetabular impingement as a cause of early osteoarthritis of the hip. *The Journal of bone and joint surgery. British volume.* 2005 Jul;87(7): 1012-1018.
14. Peters, C. L., Erickson, J. A., Anderson, L., Anderson, A. A., Weiss, J. Hip-preserving surgery: understanding complex pathomorphology. *J Bone Joint Surg*

- Am. 2009 Nov;91 Suppl 6: 42-58.
15. Tannast, M., Kubiak-Langer, M., Langlotz, F., Puls, M., Murphy, S. B., Siebenrock, K. A. Noninvasive three-dimensional assessment of femoroacetabular impingement. *J Orthop Res.* 2007 Jan;25(1): 122-131.
 16. Beck, M., Leunig, M., Parvizi, J., Boutier, V., Wyss, D., Ganz, R. Anterior femoroacetabular impingement: part II. Midterm results of surgical treatment. *Clin Orthop Relat Res.* 2004 Jan(418): 67-73.
 17. Mardones, R. M., Gonzalez, C., Chen, Q., Zobitz, M., Kaufman, K. R., Trousdale, R. T. Surgical treatment of femoroacetabular impingement: evaluation of the effect of the size of the resection. *Surgical technique. J Bone Joint Surg Am.* 2006 Mar;88 Suppl 1 Pt 1: 84-91.